[1]W. G. V. Rosser, Contemp. Phys. **1**, 453 (1960); *An Introduction to the Special Theory of Relativity* (Butterworths, London, 1964), Chap. 7.
[2]P. C. Shedd, *Fundamentals of Electromagnetic Waves* (Prentice-Hall, New York, 1954), Chap. 24.
[3]E. M. Purcell, *Electricity and Magnetism* (McGraw-Hill, New York, 1965), Chap. 7.
[4]J. R. Tessman, Am. J. Phys. **34**, 1048 (1966).
[5]W. G. V. Rosser, *Classical Electromagnetism via Relativity* (Plenum, New York, 1968), Chap. 4.
[6]A. M. Portis, *Electromagnetic Fields* (Wiley, New York, 1978), p. 707.
[7]L. A. Beauregard, Am. J. Phys. **35**, 439 (1967).
[8]R. Resnick, *Introduction to Special Relativity* (Wiley, New York, 1968), Chap. IV.
[9]Portis, Ref. 6, Chap. 11.
[10]Charge invariance need not be assumed, but may be deduced as a necessary part of electromagnetic theory. On substituting Eqs. (1) and (1') into Eq. (2), put $v = 0$ to obtain $qE_{\|} = q'E'_{\|}$, with q' now denoting charge at speed u and q denoting rest charge. In order that test charge and field components be physically independent quantities, however, the ratio q'/q can be at most a function of u. Putting $q' = qf(u)$, employing the inverse relationship $q = q'f(u)$, and requiring $f(0) = 1$ then yields $f(u) = 1$. This implies $q' = q$ for all u, that is, charge invariance.
[11]For evidence of charge invariance in an elementary experiment, see M. S. Steinberg, Am. J. Phys. **39**, 582 (1971).

Elastic electron-atom collision effects in the Franck–Hertz experiment

D. R. A. McMahon
Research School of Physical Sciences, Australian National University, Canberra, 2600, Australia

(Received 4 March 1982; accepted for publication 25 January 1983)

In the Franck–Hertz experiment one observes the effect of inelastic collisions in which fixed quanta of energy are exchanged between electrons and atoms. It is shown here that one can also readily demonstrate with a Franck–Hertz apparatus energy-dependent features of the elastic collision cross section. For mercury vapor of sufficiently high pressure, elastic electron–atom collisions between the grid and the anode are able to energy analyze the electrons so that the characteristic peaks and troughs in the anode current are still observed without the traditional retarding field to separate off the lowest-energy electrons. This is because in mercury vapor the most energetic electrons have the longest mean free path, are more penetrating through the gas, and are the most likely electrons to reach the anode. The electron transport theory for this effect is developed and applied to a crude determination of the electron energy distribution. Not surprisingly, the electron energy distribution in this experiment consists of two electron groups separated in energy by 4–5 eV consistent with the known 6^1S-6^3P energy-level separation in mercury of 4.9 eV.

I. INTRODUCTION

The original experiment of Franck and Hertz[1,2] was carried out with mercury vapor and led to two conclusions.

(i) Electrons accelerated from a hot platinum wire cathode lose energy in fixed amounts of 4.9 eV.[1]

(ii) The loss of this energy by electrons coincides with the emission from the vapor of 2537-Å uv radiation.[2]

As noted by Franck and Hertz, the observed energy loss $\Delta\epsilon$ is related to the frequency ν of emitted radiation by the Planck relation $\Delta\epsilon = h\nu$ thereby providing for the first time a definitive demonstration of Planck's postulate for isolated atoms. Detailed accounts of the historical background and discussions of the significance of this experiment for the theory of atomic structure can be found in the Nobel Lectures[3] and in the books by Millikan[4] and Trigg.[5]

The standard undergraduate teaching experiment is usually only concerned with conclusion (i), the detection of the energy losses of the electrons due to inelastic electron–atom collisions. A Leybold–Franck–Hertz apparatus which has been fully described in the literature[6–8] is used in our observations (see Fig. 1). Electrons that are accelerated by V_{G_2} from the cathode K and suffer inelastic collisions with gas atoms near G_2 are mostly collected by G_2 causing equally spaced peaks and troughs in the anode current I_A as V_{G_2} is increased (see Fig. 2). Normally a potential difference V_R is maintained between G_2 and A so that an electron which has undergone an inelastic collision close to G_2 has insufficient energy to reach A. A typical description of the Franck–Hertz experiment[6–8] draws attention to the retarding potential difference between the grid and the anode. However this retarding potential is not necessary if the vapor pressure is sufficiently high, say 10–20 Torr, as is the

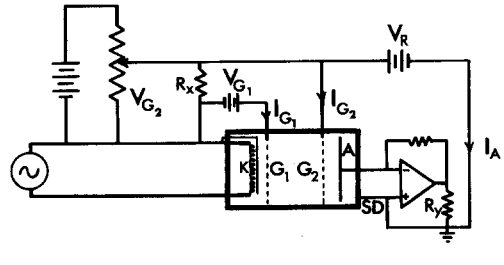

Fig. 1. Circuit diagram for the Franck–Hertz experiment. Electrons from the cathode K are accelerated by the voltage V_{G_2} and collected by grid G_2 and anode A. G_1 is a current control grid and SD is an earthed shield surrounding the electrons tube.

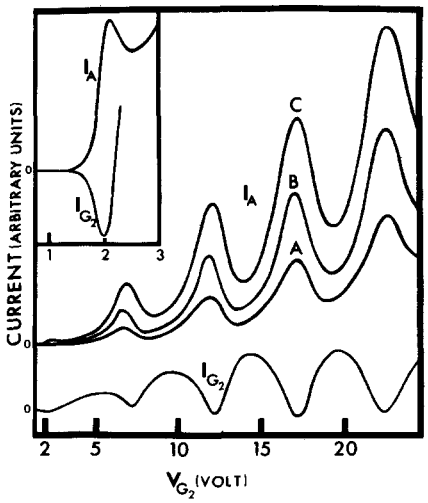

Fig. 2. Various demonstrations of the strong influence of the energy dependence of the electron mean free path in mercury vapor in the Franck–Hertz experiment. Plots of I_A vs V_{G_2} are for $-V_R = 0.5$ and 15 V for curves A, B, and C, respectively. The insert shows I_A for $V_{G_2} < 3$ V and $-V_R = 30$ V. It reveals another peak not observed under retarding field conditions between G_2 and A. Plots of I_{G_2} show minima at values of V_{G_2} peaks. The very prominent features of I_{G_2} are attained using $-V_R = 47$ V which can produce negative going currents by electron impact ionization of mercury atoms between G_2 and A.

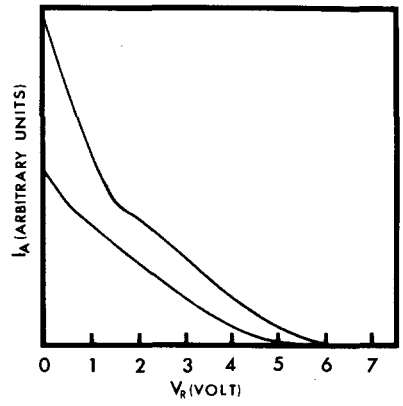

Fig. 4. I_A vs V_R for $V_{G_2} = 6.5$ V (lower curve) and $V_{G_2} = 7.3$ V (upper curve). The upper curve corresponds to a peak in the I_A vs V_{G_2} curve.

case with the Leybold apparatus used here. This is easily demonstrated by applying an accelerating potential difference for electrons between G_2 and A and observing that the usual peaks and troughs in I_A due to the presence of inelastic collisions still occur (see Fig. 2, curves A, B, and C).

An understanding of the origin of this effect requires a knowledge of the energy dependence of the electron mean free path in mercury vapor and a consideration of the theory of electron drift and diffusion in gases. The quantitative theory of electron transport in gases between two closely spaced electrodes has its origins in the work of Hertz[9] and Langmuir.[10] The latter author has shown that for zero electric field between the electrodes the probability of an electron starting at one electrode and reaching the other electrode is proportional to the electron mean free path. Figure 3 shows the electron mean free path in mercury vapor at 20 Torr taken from the momentum transfer cross-section measurements of Elford.[11] A pronounced minimum (corresponding to the maximum cross section $\simeq 180$ Å^2) is observed at 0.5 eV. Because the inelastic cross section is finite (about two orders of magnitude smaller than the elastic cross section)[12] a significant proportion of the electrons reach energies of 1 eV or more above the 6^1S–6^3P 4.9-eV threshold (see Figs. 4 and 5). Hence after undergoing inelastic collisions most electrons end up with energies somewhere near the minimum in the mean free path. It follows from Langmuir's result that these electrons are much less penetrating through the gas than those at higher energies and so are more readily captured by the grid G_2. This removes the lowest-energy electrons and consequently one still observes the usual rises and falls in anode current without a retarding field between G_2 and A. The extension of Langmuir's results to allow for both a nonzero electric field and an energy-dependent mean free path is presented in Sec. III. Section IV shows how to obtain the approximate energy distribution (Fig. 5) for electrons arriving at G_2.

The main objective of this paper is to draw to the atten-

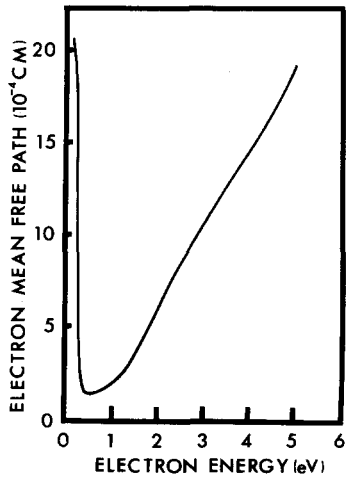

Fig. 3. Mean free path $l(\epsilon)$ for electrons in mercury vapor at 20 Torr vs electron energy calculated from $l(\epsilon) = [Nq_m(\epsilon)]^{-1}$, where N is the number density of the mercury atoms and $q_m(\epsilon)$ is the momentum transfer cross section (data of Elford, Ref. 11).

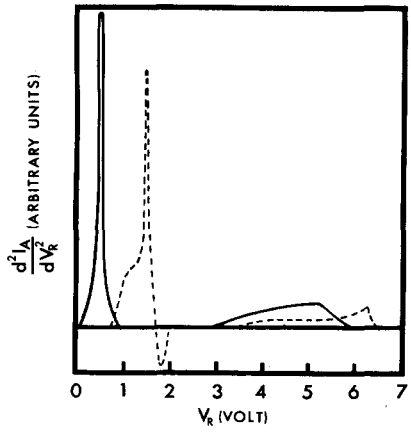

Fig. 5. The second derivative of I_A with respect to V_R for the two curves shown in Fig. 4. The plotted quantity approximates the electron energy distribution in our experiment. The two energy groups indicated by the plots shift by the correct amount when V_{G_2} is changed. Full curves, $V_{G_2} = 6.5$ V. Dashed curves, $V_{G_2} = 7.3$ V.

tion of physics instructors the conditions for and nature of elastic electron–atom collision influences on the Franck–Hertz experiment. A situation that could easily arise in a teaching laboratory is as follows. A student may make a "mistake" by connecting the terminals for the dc supply V_R the "wrong" way around (so that electrons are accelerated from G_2 to A). The student may be sharp enough to see the need for an explanation why the Franck-Hertz experiment continues to work. Because the standard discussion in the literature is not accompanied with information on the energy dependence of the electron mean free path in mercury vapor (and the relevant transport theory) both the student and the instructor may be mystified by the phenomenon. Physics teachers to whom the author has pointed out this effect were surprised. Although the relevant theoretical principles are well established from studies of electron transport in gases[13] the author has not found in the literature any explicit reference to the effect of an energy-dependent mean free path on this experiment. This is possibly because the experimental systems of Franck and Hertz and others use much lower vapor pressures than our Leybold apparatus so that the electron mean free path is too long for whatever grid–anode separation is employed to show the mean-free-path effect.

A secondary objective of the paper is to show how a Franck–Hertz apparatus can be used to demonstrate in a particularly simple manner a particle transport phenomenon sensitive to the mean free path. This contrasts with, for instance, measurements of the coefficients for gas diffusion, thermal conductivity, and viscosity, where the connections with the mean free path given by kinetic theory[14,15] are much more indirect. These observations with a Franck–Hertz apparatus are also instructive by showing that the mean free path can be strongly energy dependent, a point often omitted in many elementary discussions of the mean free path.[14–16]

II. EXPERIMENT

Our experiment employs a 55580 Leybold–Franck–Hertz electron tube.[6–8] The electron accelerating voltage V_{G_2} and the current I_A are conveniently recorded with an X-Y plotter as described by Carpenter[17] (see Fig. 1). The electron tube containing spectroscopically pure mercury is heated in an oven to give an estimated vapor temperature of 205 ± 5 °C and so a vapor pressure of about 20 Torr. To avoid excessive accumulated energy losses by elastic electron–atom collisions the surfaces of the cathode K and the grid G_2 are separated by 7.2 mm in contrast with 40 mm in the case of the original apparatus of Franck and Hertz which operated with much lower vapor pressures near 1 Torr.

As already discussed, curves A, B, and C of I_A vs V_{G_2} shown in Fig. 2 demonstrate that the Franck–Hertz experiment continues to work even for a strong electron accelerating electric field between G_2 and A. For completeness the variation of I_{G_2} with V_{G_2} is also shown. Each peak in I_A coincides with a minimun in I_{G_2} and vice-versa. The sum $I_A + I_{G_2}$ (not shown) is a smoothly increasing function of V_{G_2} and is relatively insensitive to V_R. There is a somewhat surprising improvement in resolution for strong accelerating voltages V_R. The insert in Fig. 2 demonstrates this by revealing another peak in I_A (and minimum in I_{G_2}) only observed in our experiment under strong electron accelerating conditions between G_2 and A.[18] A possible reason for this is that the fastest electrons arriving at the G_2–A region dominate both I_A and the ionization process $\mathrm{Hg} + e \rightarrow \mathrm{Hg}^+ + 2e$ (produced by the electron accelerating voltage between G_2 and A) so that a current avalanche, which enhances the anode current by the greatest amount near the peaks of I_A, is produced. The existence of ionization between G_2 and A is readily verified by measuring I_{G_2} which can be made to reverse sign near the minima due to the positive ion current (see the insert of Fig. 2).

It is possible to obtain a crude scan of the energy distribution function for electrons arriving at G_2 from K. Figure 4 shows a plot of I_A versus the retarding potential V_R for two values of V_{G_2}. The approximate energy distribution is shown in Sec. IV to be given by the second derivative of I_A with respect to V_R (see Fig. 5). The theory behind this requires that the electron mean free path $l(\epsilon)$ be linearly proportional to the electron energy ϵ. As can be seen from Fig. 3 this is only approximate above 0.5 eV. It is also assumed that the electron reflection probability of G_2 is not strongly energy-dependent. The errors in these approximations are believed to result in the small negative part of the "distribution function" and probably also contribute to the apparent spread in the higher-energy component. Nevertheless Fig. 5 shows, as one would expect, two groups of electrons differing in energy by 4–5 eV, consistent with the known inelastic collision energy exchange of 4.9 eV. As a check curves have been obtained for two values of V_{G_2} differing by 0.8 V and Fig. 5 shows that the two components of the distribution function are both shifted by about the expected amount 0.8 eV.

Figure 6 shows $I_A/(I_A + I_{G_2})$ as a function of the estimated vapor pressure. A systematic study of the internal temperature of a nonoperational Franck–Hertz electron tube enabled estimates of the vapor temperature to be made from the oven temperature and filament heater voltage. In obtaining Fig. 6, V_{G_2} was fixed at 15 V and I_A/I was measured as the apparatus slowly cooled. The results are qualitatively consistent with the theory of Secs. III and IV which predicts both the strong dependence of I_A/I on the vapor pressure observed near our normal operating pres-

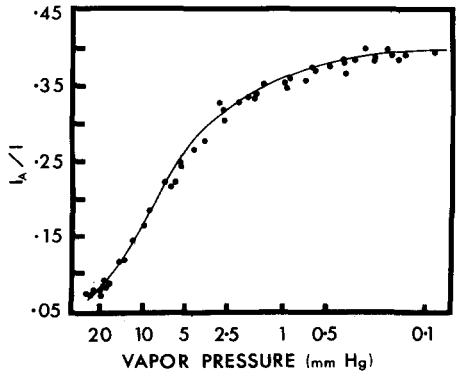

Fig. 6. Effect of electron–mercury atom collisions on the anode current as a fraction of the total current $I = I_A + I_{G_2}$. The vapor pressure is obtained from estimated vapor temperatures. The low-pressure region shows the theoretically expected behavior where the current ratio I_A/I saturates to a constant value (0.4) independent of the vapor pressure.

sure 20 Torr (and much lower pressures) and the low-pressure saturation of I_A/I to a constant value. Although our theory becomes quantitatively inaccurate at low pressures where the electron mean free path becomes comparable with the G_2–A separation the theory improves on Langmuir's theory[10] which does not give the low-pressure saturation behavior of I_A/I.

III. THEORY OF THE ELECTRON FLUX BETWEEN CLOSELY SPACED ELECTRODES

Rather than go through the full derivation of the flux density Γ (number of electrons s^{-1} m^{-2}), which is given elsewhere[19] in a generalization of the work of Hertz[9] and Langmuir,[10] we quote an intermediate equation which happens to be understandable in elementary terms anyway. This equation is

$$\Gamma = \frac{1}{3}\frac{eEl(z)}{mc(z)}n(z) - \frac{c(z)l(z)}{3}\frac{dn(z)}{dz}, \tag{1}$$

where $n(z)$ is the electron number density, m is the mass of the electron, E is the electric field strength, $c(z)$ is the electron speed, and $l(z)$ is the mean free path. It is possible to parametrize the electron energy, speed, and mean free path as functions of the coordinate z along the electric field direction because of the approximate energy conservation relation $\epsilon(z) = \epsilon(z_0) + eE(z - z_0)$ for electrons scattered elastically from the heavy gas atoms. The justification for this approximation is that an electron (mass m) only loses an average fraction ($2m/M \simeq 5 \times 10^{-6}$) of its energy in an elastic collision with a mercury atom (mass M) and the characteristic distance scale $l_\epsilon = (M/2m)^{1/2}l$ for the loss of a significant proportion of the initial energy is much larger than the G_2–A separation $L \simeq 2$ mm. For instance, for 5-eV electrons in mercury vapor of pressure 20 Torr, l_ϵ is about 10 mm.

The coefficient $\frac{1}{3}eEl/mc$ on the right-hand side of Eq. (1) multiplying $n(z)$ is the electron drift velocity and, except for the numerical factor $\frac{1}{3}$, agrees with elementary mean-free-path expressions.[14,15] The second term on the right-hand side represents electron diffusion with a diffusion coefficient $lc/3$ which agrees with the mean-free-path result.[14,15] Aside from the omission of energy losses by elastic collisions, a number of other approximations are implicit in the derivation of Eq. (1) and its application to electron transport between G_2 and A. The Lorentz two-term approximation is used where the distribution function $f(\mathbf{r},\mathbf{c})$ is written as $f_0(z,c) + f_1(z,c)\cos\theta$, where $\mathbf{c}\cdot\mathbf{E} = -cE\cos\theta$.[13] This approximation fails if f_1 is not small compared with f_0. Its consistency can easily be checked at the end of the theoretical calculation. Also implicit is the neglect of the atomic speeds in comparison with the electron speeds. We also require l much less than the G_2–A separation which from Fig. 3 is clearly valid for our case. Inelastic collisions between G_2 and A are neglected so that it is assumed that most inelastic collisions occur before the electrons enter the region between G_2 and A. The effect of inelastic collisions on electron transport between closely spaced electrodes is discussed in a more specialist report elsewhere.[19] Further, because the K–G_2 radius is much larger than the separation between G_2 and A the G_2–A system has been approximated as plane-parallel electrodes rather then cylindrical. Finally, the mesh of G_2 is considered to be sufficiently fine for G_2 to be treated as a plane electrode with some effective electron reflection probability.

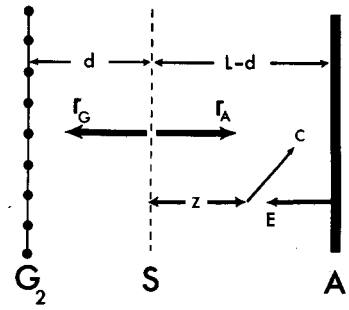

Fig. 7. The theoretical analysis considers a system where electrons are emitted isotropically from a source S at distance d from G_2 and distance $L - d$ from A. Because all electrons arriving from the cathode must pass through the plane of G_2 and must ultimately be absorbed by G_2 or A, the theory represents our experiment when we set $d = 0$. The electron fluxes Γ_A and Γ_G are calculated by solving Eq. (1) with appropriate boundary conditions for the electron number density at A, G_2, and S. Equation (1) is derived from the "two-term" approximation which assumes at all z a $\cos\theta$ deviation from isotropy of the distribution of electron velocities c.

If we convert to the energy variable ϵ for the moment and write

$$n(\epsilon) = n_S\left(\frac{\epsilon}{\epsilon_S}\right)^{1/2}p(\epsilon), \tag{2}$$

then Eq. (1) becomes

$$\Gamma = -\frac{2eEl(\epsilon)n_S}{3mc_S}\epsilon\frac{dp(\epsilon)}{d\epsilon}. \tag{3}$$

Here n_S, ϵ_S, and c_S are the electron number density, energy, and speed at a source of monoenergetic electrons between G_2 and A of strength Γ_S electrons per unit area per second. Let the source be idealized as a plane-parallel source at a distance d from G_2 (see Fig. 7). In the final application of the theory d is considered to be much less than L in order to simulate the arrival at the grid of electrons from the cathode K. For the moment we distinguish two fluxes Γ_A and Γ_G, where $\Gamma_G + \Gamma_A = \Gamma_S$. We now solve for Γ_A and the corresponding result for Γ_G follows in the same way.

Because Γ_A is independent of z, Eq. (3) can be solved to give

$$p(\epsilon) = 1 - \frac{3\Gamma_A mc_S}{2eEn_S}\int_{\epsilon_S}^{\epsilon}\frac{d\epsilon'}{\epsilon' l(\epsilon')}. \tag{4}$$

To progress further, electrode boundary effects need to be introduced. Provided that A is not too highly reflective of electrons, it turns out that the final expression for Γ_A is not sensitive to the electrode surface properties but is dominated by electron–atom collisions. Elementary gas kinetic theory shows that in the absence of a net flow the flux of electrons incident onto a wall or electrode plane is just $nc/4$.[14] We define an absorption coefficient α_A for the anode such that

$$\Gamma_A = \alpha_A(n_A c_A/4). \tag{5}$$

Normally we would expect α_A to have the upper limit of unity; however, when Γ_A and α_A are defined carefully taking into account the net flow of electrons when calculating the flux incident onto A, it is found that α_A can be as large

as two.[19] In terms of the reflection probability r_A we find

$$\alpha_A = 2(1 - r_A)/(1 + r_A) .$$

Possible energy changes by electrons reflected inelastically from the anode are ignored. Combining Eqs. (2) and (5) we find

$$\Gamma_A = \alpha_A (c_A^2 n_S / 4c_S) p_A . \tag{6}$$

Substituting Eq. (6) into Eq. (4) and setting $\epsilon = \epsilon_A$, p_A can be extracted immediately and is given by

$$\frac{1}{p_A} = 1 + \frac{3\alpha_A \epsilon_A}{4eE} \int_{\epsilon_S}^{\epsilon_A} \frac{d\epsilon'}{\epsilon' l(\epsilon')} . \tag{7}$$

Expressions analogous to Eqs. (6) and (7) also apply to Γ_G.

To express Γ_A and Γ_G in terms of Γ_S we apply the continuity equation

$$\Gamma_A + \Gamma_G = \Gamma_S . \tag{8}$$

Combining Eq. (6), its equivalent for Γ_G, and Eq. (8) we have

$$\frac{n_S}{2mc_S} = \frac{\Gamma_S}{\alpha_A \epsilon_A p_A + \alpha_G \epsilon_G p_G} . \tag{9}$$

Finally substituting Eq. (9) into Eq. (6) leads to

$$\Gamma_A = \frac{\Gamma_S}{1 + \alpha_G \epsilon_G p_G / \alpha_A \epsilon_A p_A} , \tag{10a}$$

and

$$\Gamma_G = \frac{\alpha_G \epsilon_G p_G}{\alpha_A \epsilon_A p_A} \Gamma_A . \tag{10b}$$

IV. DISCUSSION OF THEORETICAL AND EXPERIMENTAL RESULTS

Rather than deal with flux densities we convert to actual currents I_A and $I = I_A + I_G$ in place of Γ_A and Γ_S. Further, we need to introduce a distribution of electron energies. For simplicity we set $d = 0$ (and hence $p_G = 1$) and treat the effective source S (representing the electrons from the cathode reaching the grid region) as if situated in the place of the grid. Γ_A/Γ_S given by Eq. (10a) is essentially the probability of an electron starting at the source being eventually absorbed at the anode. Simply weighting this probability over the distribution of electron energies at the source gives the general expression for the flux. Consider a retarding field to exist between G_2 and A. We find

$$I_A(\epsilon_m) = \int_{\epsilon_m}^{\infty} J(\epsilon) \left(1 + \frac{\alpha_G \epsilon}{\alpha_A \epsilon_A} \frac{1}{p_A}\right)^{-1} d\epsilon , \tag{11a}$$

where

$$J(\epsilon) = \frac{dI(\epsilon)}{d\epsilon} . \tag{11b}$$

Here ϵ_m (equal to eV_R) is the energy at the grid required for electrons to just reach A with energy $\epsilon_A = 0$. Thus for electrons with energy ϵ at G_2, $\epsilon_A = \epsilon - \epsilon_m$. When I_A/I is dominated by electron–atom collisions Eq. (11a) can be approximated by

$$I_A(\epsilon_m) \simeq \frac{4}{3} \frac{1}{L} \int_{\epsilon_m}^{\infty} \frac{1}{\alpha_G(\epsilon)} J(\epsilon) \times \frac{\epsilon_A - \epsilon}{\epsilon} \left(\int_{\epsilon}^{\epsilon_A} \frac{d\epsilon'}{\epsilon' l(\epsilon')} \right)^{-1} d\epsilon , \tag{12}$$

where eE has been eliminated using $eEL = \epsilon_A - \epsilon$. A general energy-dependent absorption coefficient $\alpha_G(\epsilon)$ is assumed for the grid.

In the limit $E \to 0$, Eq. (12) becomes

$$I_A(0) \simeq \frac{4}{3} \frac{1}{L} \int_0^{\infty} \frac{1}{\alpha_G(\epsilon)} J(\epsilon) l(\epsilon) \, d\epsilon . \tag{13}$$

Equation (13) can be written as

$$I_A(0) \simeq \frac{4}{3} \frac{1}{L} I \left\langle \frac{l(\epsilon)}{\alpha_G(\epsilon)} \right\rangle , \tag{14}$$

where the brackets denote the current density distribution weighted average. This bracket is roughly a function of the mean energy $\bar{\epsilon}$ of the distribution. In order to explain why $I_A(0)$ exhibits the strong periodic dependence on V_{G_2} and therefore on $\bar{\epsilon}$ (see curve A of Fig. 2), whereas I is only a slow, monotonically increasing function of V_{G_2}, it is necessary for $l(\epsilon)/\alpha_G(\epsilon)$ to be strongly energy-dependent. This is just as expected from the known behavior of $l(\epsilon)$ shown in Fig. 3.

Suppose that $l(\epsilon) = l'\epsilon$, as is approximately valid for mercury vapor for energies above 0.5 eV. Then Eq. (12) becomes

$$I_A(\epsilon_m) \simeq \frac{4}{3} \frac{l'}{L} \int_{\epsilon_m}^{\infty} \frac{J(\epsilon)}{\alpha_G(\epsilon)} (\epsilon - \epsilon_m) \, d\epsilon . \tag{15}$$

Differentiating twice we have

$$\frac{d^2 I_A(\epsilon_m)}{d\epsilon_m^2} \simeq \frac{4}{3} \frac{l'}{L} \frac{J(\epsilon_m)}{\alpha_G(\epsilon_m)} . \tag{16}$$

Assuming $\alpha_G(\epsilon)$ is not strongly energy-dependent we see from Eq. (16) that the prominent peaks in the second derivative of I_A, with respect to the retarding potential shown in Fig. 5, indicate peaks in the electron energy distribution.

It is interesting to estimate what proportion of the electrons exists in each peak of Fig. 5 and how much of the anode current each peak in the electron energy distribution contributes to I_A for say $V_R = 0$. Let us idealize the energy distribution as two δ functions at energies ϵ_1 and ϵ_2 and let us assume that α_G is roughly constant. We can then write Eq. (14) as

$$I_A \simeq \frac{4}{3} \frac{l'}{L\alpha_G} (\epsilon_1 I_1 + \epsilon_2 I_2) , \tag{17}$$

where I_1 and I_2 are the two separate energy range contributions to I. I_1 and I_2 are proportional to the areas under the peaks in Fig. 5. Our analysis for $V_{G_2} = 6.5$ V shows that the higher energy peak accounts for 60% of the electrons in I but is responsible for 90% of the anode current. At $V_{G_2} = 7.3$ V, the higher energy peak has declined to 25% of all electrons in the net current I but is still responsible for 60% of I_A. These results emphasize the fact that the higher-energy electrons are much more penetrating through the gas and can contribute most of the anode current even though they represent a minority of the electrons reaching the grid–anode region. The above observations were repeated with a second Franck–Hertz tube. Somewhat lower ($\simeq$10%) percentages were obtained at equal voltage conditions so that actual results appear to be very sensitive to slight differences in the electrodes. V_{G_1} has a marked effect

also by influencing the distribution of inelastic collisions with distance between G_1 and G_2, particularly for V_{G_1} above 5 V where inelastic collisions near G_1 can shift the anode current peak positions and change the two relative populations in the electron energy distribution.

One might believe that an estimate of the absolute value of the electron mean free path can be made using the Franck–Hertz experiment and the common assumption[20] that most electrons incident onto an electrode surface are not reflected ($\alpha_G \simeq 2$).[21] However the assumption $\alpha_G \simeq 2$ is incorrect because by using Eq. (16) and Fig. 3 to estimate l' we find for our experiment $\alpha_G \simeq 0.1$. This same conclusion also follows from Eq. (11a) and Fig. 6 using the observation that I_A/I only changes by one order of magnitude over the pressure range used, even though the mean free path changes by two orders of magnitude. The grid wires are highly reflective of electrons causing the anode current to be an order of magnitude larger in our experiment at 20 Torr than otherwise expected.

V. SUMMARY

The formation of the usual peaks and troughs in the anode current in the Franck–Hertz experiment with mercury vapor of sufficiently high pressure does not require a retarding electric field between the grid and anodes. Although the Franck–Hertz experiment is widely performed in student laboratories, this phenomenon and its underlying physical origin are not widely know to the physics teaching community. The relevant electron transport theory has been applied to show that this phenomenon arises from the strong energy dependence of the electron mean free path in mercury vapor. The energy dependence of the electron mean free path is of interest in its own right and can easily be demonstrated in the student laboratory using a gas-filled electron tube with a closely spaced grid and anode system. To complete the demonstration of the electron drift and diffusion effects in the Franck–Hertz experiment, we have related the grid–anode retarding voltage dependence of the anode current to the approximate electron energy distribution and verified that two energy groups of electrons exist with a separation in energy consistent with the known inelastic collision energy exchange of 4.9 eV. We believe that our discussion provides physics instructors with a useful and previously unavailable background knowledge of electron elastic collision and transport effects in the Franck–Hertz experiment.

[1] J. Franck and G. Hertz, Verh. Dtsch. Phys. Ges. **16**, 457 (1914) [English translation, *World of the Atom*, edited by H. A. Boorse and L. Motz (Basic Books, New York, 1966), Vol. I, pp. 770–778].

[2] J. Franck and G. Hertz, Verh. Dtsch. Phys. Ges. **16**, 512 (1914).

[3] *Nobel Lectures, Physics, 1922–1941* (Elsevier, Amsterdam, 1965), pp. 98–129.

[4] R. A. Millikan, *Electrons (+ and −), Protons, Photons, Neutrons, Mesotrons and Cosmic Rays* (Univ. Chicago Press, Chicago, 1947), Chap. X.

[5] G. Trigg, *Crucial Experiments in Modern Physics* (van Nostrand Reinhold, New York, 1971; also Crane, Russak and Co., New York, 1975).

[6] Leybold–Heraeus Physics Leaflet D. C. No. 535, 35a (1959).

[7] A. C. Melissinos, *Experiments in Modern Physics* (Academic, New York, 1966), p. 8.

[8] *Physics Demonstration Experiments*, edited by H. F. Meiners (Ronald Press, New York, 1970), Vol. II, p. 1210.

[9] G. Hertz, Phys. **32**, 278 (1925).

[10] I. Langmuir, Phys. Rev. **38**, 1656 (1931).

[11] M. T. Elford, Aust. J. Phys. **33**, 231 (1980); **33**, 251 (1980).

[12] H. S. W. Massey and E. H. S. Burhop, *Electronic and Ionic Impact Phenomena* (Oxford U. P., London, 1969), Vol. I, pp. 216–22.

[13] L. G. H. Huxley and R. W. Crompton, *The Diffusion and Drift of Electrons in Gases* (Wiley, New York, 1974).

[14] R. D. Present, *Kinetic Theory of Gases* (McGraw-Hill, New York, 1958).

[15] E. H. Kennard, *Kinetic Theory of Gases* (McGraw-Hill, New York, 1938).

[16] D. Halliday and R. Resnick, *Fundamentals of Physics* (Wiley, New York, 1974), pp. 391–393, 514–516.

[17] K. H. Carpenter, Am. J. Phys. **43**, 190 (1975).

[18] A peak in I_A for $V_{G_2} \simeq 2.0$ V is somewhat surprising. It implies a large cathode–grid contract potential of about 3 V. But a peak at $V_{G_2} \simeq 2.0$ V means that the cathode must have a work function which is 3 eV higher than that to of G_2. In view of the fact that G_2 consists of nickel (clean surface work function $\simeq 5.0$ eV) and that the cathode is an indirectly heated [Ba Sr]O thermionic emitter commonly used in electron tubes because of the very low work function (less than 2.0 eV) the observed contact potential suggests that the cathode and electrode work functions are strongly affected by contaminants of unknown origin. For an elementary discussion of contact potentials and the effects of surface contaminants, see F. A. Vick in *Encyclopaedic Dictionary of Physics*, edited by J. Thewlis (Pergamon, New York, 1961), Vol. 2, p. 62.

[19] D. R. A. McMahon, Aust. J. Phys. **36**, 27 (1983); *ibid.* **36**, 45 (1983).

[20] E. W. McDaniel, *Collision Phenomena in Ionized Gases* (Wiley, New York, 1964), pp. 496–497.

[21] I_{G_2} can be related to the local random flux $n_G c_G/4$, the total surface area of the grid wires and the electron reflection probability of the grid wires. Because the surface area of the grid wires is almost equal to the effective area of the grid treated as an electrode with a plane surface, the effective absorption coefficient of the grid is $\alpha_G \simeq 2$ if the grid wires do not reflect electrons.

PROBLEM: AN N-DEGREE-OF-FREEDOM VIBRATING SYSTEM WITH A SINGLE NATURAL FREQUENCY

Consider the system shown in Fig. 1, which has four degrees of freedom, x_1, x_2, x_3, and x_4. Each particle of mass $m = 1$ is connected by springs of constant $k = 1$ to each of the other particles. The springs are undeflected when the displacements are zero, and motion is constrained to be in the horizontal direction. Find the equations of motion of the system. Generalize the result to n particles. Find the natural frequencies of vibration. (Solution is on page 1161.)

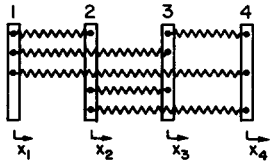

Fig. 1. System of particles.

E. Wilms
H. Cohen
University of Manitoba
Winnipeg, Canada